CONSTRUCTION
E-ISSN: 2785-8731
VOLUME 6, ISSUE 1, 2026, 113 - 126
DOI: https://doi.org/10.15282/construction.v6i1.13691

RESEARCH ARTICLE

Advanced retaining wall using reinforced soil block and rubber backfill incorporated IoT monitoring system

Zaffri Zaki[1], Nik Norsyahariati Nik Daud[1]*, Muhammad Zulhafizi Muhammad Zuraidi[1], Abdullah Iman Sahatim[1], Abubakar Sadiq Muhammed[2]

[1]Department of Civil Engineering, Faculty of Engineering, Universiti Putra Malaysia, Serdang 43400, Selangor, Malaysia
[2]Department of Civil and Water Resources Engineering, University of Maiduguri, Maiduguri 600104, Borno, Nigeria

Abstract - The critical challenge in geotechnical engineering related to the construction of a retaining wall is the poor properties of native soil, which often consist of weak materials unsuitable for structural support. Consequently, the cost of importing high-quality backfill materials is frequently required. This study investigates an innovative retaining wall system developed using kenaf fiber-reinforced soil blocks and rubber-soil backfill material integrated with an Internet of Things (IoT)-based monitoring system. The objectives of the study are to evaluate the properties of kenaf fiber-reinforced soil blocks and soil-rubber backfill, and to assess retaining wall stability by incorporating a real-time environmental monitoring system. The methodology was divided into two phases; Phase 1 involved laboratory evaluation of the mechanical properties of the fiber-reinforced soil block and soil-rubber backfill, while Phase 2 focused on monitoring environmental parameters using an IoT-based Arduino system. The results showed that the kenaf fiber-reinforced soil blocks at a 0.75% concentration achieved a compressive strength of 0.96 N/mm² and a flexural strength of 0.75 N/mm², demonstrating significant improvements in load-bearing capacity and resistance to environmental degradation. Furthermore, incorporating rubber waste materials from discarded tires as backfill at optimal concentrations of 20% to 30% enhanced the flexibility, stress distribution, and hydrostatic pressure and drainage performance, as indicated by its laboratory-scale results. The IoT monitoring system enables early detection of slope conditions susceptible to landslides and soil saturation, thereby enhancing early warning capabilities. Overall, the proposed retaining wall system shows strong potential for application in infrastructure projects, particularly in areas requiring improved drainage and sustainability.

Article History
Received : 23 December 2025
Revised : 2 February 2026
Accepted : 25 February 2026
Published : 30 June 2026

Keywords
Retaining wall system
Soil block
Rubber-soil backfill
IoT monitoring
Environmental

1. Introduction

In geotechnical engineering applications, retaining wall systems play an important role in providing the structural support needed for infrastructure development, highway embankments, and slope stabilisation in challenging terrain. The performance of these systems is highly dependent on the quality of backfill materials, which must have sufficient strength, drainage capabilities and long-term stability to maintain structural integrity. Conventional retaining systems typically consist of rigid walls filled with granular, cohesionless soil owing to the well-established engineering properties of this soil [1]] – [[2]. The stability of the retaining wall can be enhanced and its lateral earth pressure on the wall reduced by mechanically connecting a geogrid-reinforced backfill to the retaining wall face [3]. Despite these advantages, conventional retaining wall systems pose significant environmental and economic concerns that require innovative, sustainable solutions. The construction industry is facing substantial pressure to identify alternative backfill materials due to the depletion of high-quality natural aggregates and the rising materials cost [2]. In addition, traditional backfill materials such as sand and gravel have long been preferred for their reliable mechanical properties and proven performance [4]. However, global emphasis on sustainable construction has encouraged the adoption of environmentally friendly materials as substitutes for conventional aggregates. The selection of suitable backfill materials is influenced by several factors, including permeability, unit weight, long-term durability, and shear strength parameters. Cohesionless materials with high internal friction angles are particularly effective in reducing lateral earth pressures and ensuring efficient drainage behind the wall face [5]. To preserve environmental ecosystems, using tyre waste as backfill material can be advantageous for soil reinforcement. In Malaysia, an estimated 8.2 million waste tyres, equivalent to 57391 tonnes, reach the end of their usable lives annually [6]. In recent years, the application of waste tyres in geotechnical engineering, particularly in soil reinforcement, has gained significant attention [7]. Studies have shown that sand-tire chip mixtures can significantly reduce construction costs while decreasing lateral earth pressures and horizontal displacements by 50-60% compared to conventional sand backfill [2]. Mixtures containing up to 20% coarse-grained tire-chips and 30% fine-grained tire-chips have been reported to enhance shear strength characteristics [8].

Conventional soil blocks have become a key component in sustainable construction due to their cost-effectiveness and environmental benefits. However, their production often relies on high cement content, which contributes significantly to carbon dioxide emissions. The cement industry accounts for approximately 8% of global CO_2 emissions, highlighting the urgent need for sustainable alternatives [9]] – [[10]. The fibre from the Hibiscus cannabinus plant, which is known as kenaf, has significant potential for use in geotechnical applications. Kenaf fibres, which are derived from the bast of the Hibiscus Cannabinus plant, are composed of cellulose (56–64 weight per cent), hemicellulose (21–35 weight per cent), and lignin (8–14 weight per cent) [11]. This fibre can be a great option for soil block reinforcement due to its high tensile

***CORRESPONDING AUTHOR | Nik Norsyahariati Nik Daud** | ✉ niknor@upm.edu.my

strength, biodegradability, and renewability. Kenaf fibres exhibit the highest carbon dioxide absorption capacity, require minimal production energy, and have a high modulus and low density among natural fibres [12]. Previous studies have reported that the inclusion of natural fibres such as kenaf and coir increases the Optimum Moisture Content (OMC) while reducing the Maximum Dry Density (MDD) of soils, thereby improving soil stability [13]. These findings highlight the importance of optimising fibre content to balance moisture content and dry density, thereby enhancing soil performance and structural integrity [13]] –[[14].

In the recent era of material innovation, slope monitoring systems have evolved from manual inspection techniques to more automated approaches. Conventional slope monitoring systems often rely on periodic measurements that may fail to capture critical changes in slope conditions and lack continuous real-time data acquisition capabilities [15]] – [[16]. Thus, an advanced system is needed to continuously monitor the environmental factors that trigger landslides. Key parameters, including temperature, humidity, surface runoff, slope angle, and soil moisture, are important in these monitoring systems. Temperature and humidity sensors detect changes in the properties of soil and water, moisture sensors determine the amount of water in the soil, and slope angles are measured to evaluate the effect of rainfall on slope stability [17]. Recent advancements in IoT technology have introduced innovative solutions for slope monitoring. These systems offer significant benefits, such as enhanced data accuracy and early detection of potential slope failures. Advancements in IoT technology have expanded the capabilities of slope monitoring systems. Innovations such as advanced sensors, improved data analytics, and enhanced communication technologies contribute to more accurate and reliable monitoring solutions [18]] – [[19]. Combining real-time data from IoT systems with traditional monitoring techniques can enhance the accuracy of infiltration modelling and slope management. Various types of sensors, including dielectric moisture sensors, pore pressure piezometers, strain gauges, tilt meters, geophones, rain gauges, and temperature sensors, are part of the sensor suite for landslide detection [20]. The aim of this study is to evaluate the performance of an innovative retaining wall system incorporating kenaf fibre-reinforced soil blocks and a soil-rubber backfill material, integrated with an IoT-based environmental monitoring system, at the laboratory scale to establish baseline performance characteristics and validate the conceptual framework for future field implementation.

2. Methods and Materials

2.1 Materials

The soil sample was retrieved and collected at Bandar Baru Nilai, 71800 Nilai, Negeri Sembilan, Malaysia (2.822474, 101.787005). The area is predominantly underlain by sedimentary rocks with a minor proportion of volcanic components. Based on the geological map legend (Figure 1), shale is the dominant rock type in the study area. The improvised backfill materials, consisting of natural soil mixed with crumb rubber tyre waste, were tested in the soil laboratory. Tire waste materials were acquired from Yong Fong Rubber Industries Sdn. Bhd. located in Malaysia. The two crumb rubber sizes used in this study, 1 to 4 mm and 5 to 8 mm, were selected to ensure optimal gradation control in the backfill mixture (Figure 2). Kenaf fibres were used in this study due to their excellent environmental properties when mixed with the soil. The samples were retrieved from Lembaga Kenaf dan Tembakau Negara, Malaysia, as shown in Figure 3. Two grades of kenaf fibre were evaluated, which are Grade A and Grade B, where the length of fibre was standardised at 30 mm to 50 mm for consistency for all test specimens.

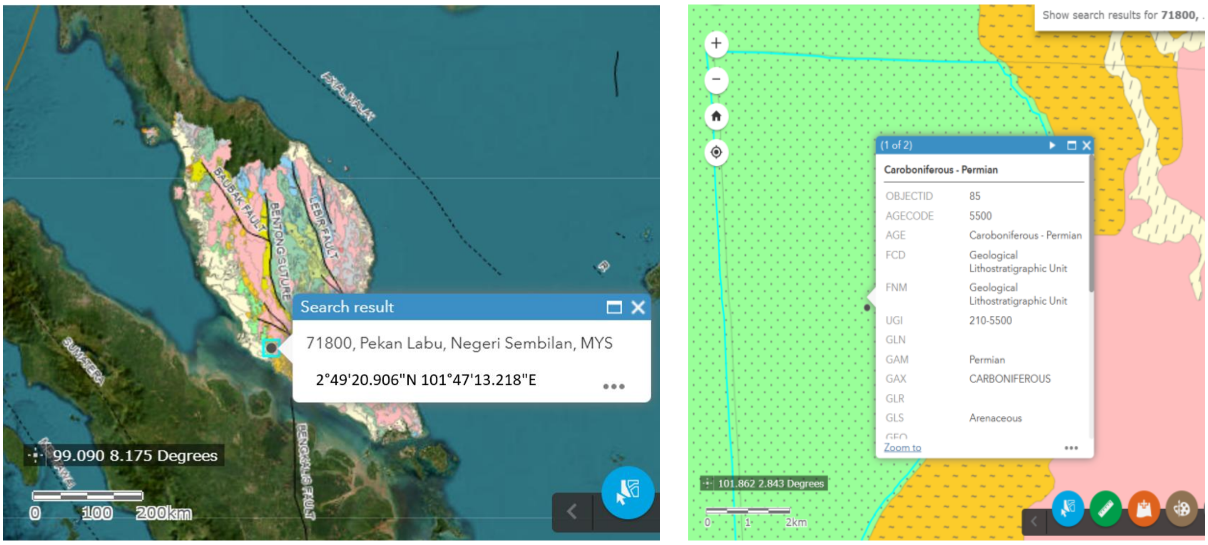

(a) (b)

Figure 1. a) Geological map of Bandar Baru Nilai, 71800 Nilai, Negeri Sembilan, Malaysia, b) the geological details of the studied area [21]

Figure 2. Sample of crumb rubber tire waste materials (1 to 4 mm and 5 to 8 mm size)

Figure 3. Sample of kenaf fiber (standardized at 30 mm to 50 mm in length)

2.2 Methodology

The experimental program was conducted in four phases: i) the determination of geotechnical properties of the natural soil, ii) evaluation of soil-crumb rubber tyre waste backfill mixture, iii) assessment of kenaf fibre-reinforced soil blocks and iv) real-time tracking of advanced retaining system monitoring using IoT sensors.

2.2.1 Geotechnical properties tests

The geotechnical properties tests were carried out in the soil laboratory and were divided into two stages: i) physical properties test, and ii) mechanical properties tests. The physical properties tests included the particle size distribution (standard: ASTM D6913-04; equipment: Endecotts EFL 2000 Sieve Shaker machine) [22]; Atterberg limits test was used to determine the liquid limit, plastic limit, and shrinkage limit of a fine-grained soil to characterize its behaviour with changing moisture content (standard: ASTM D 4318; apparatus: Casagrande set) [23]; specific gravity of the soil solids was a test to determine the parameters such density and void ratio (standard: ASTM D854-14; apparatus: pycnometer) [24]. The standard proctor compaction test was a mechanical method designed to minimise the air spaces between soil particles by bringing them closer together. This test is carried out in accordance with ASTM D698: Standard Test Methods for Laboratory Compaction Characteristics of Soil Using Standard Effort [25]. The mechanical properties of soil were assessed using strength tests, including a direct shear test (standard: ASTM D3080 – Standard Test Method for Direct Shear Test of Soils Under Consolidated Drained Conditions) [26], and permeability behaviour, assessed using a falling-head permeability test (standard: ASTM D5084) [27].

2.2.2 Crumb rubber tire waste-soil backfill material properties tests

The performance of a crumb rubber tyre waste-soil mixture as backfill material was evaluated using physical model testing. The mixture proportions were evaluated across five different mixtures: the control sample (0%) and soil mixed with 10%, 20%, 30%, and 40% crumb rubber tyre waste by weight. The selection criteria were based on three key parameters: shear strength (cohesion and friction angle), permeability, and performance in physical model testing. Physical model testing involved applying the surcharge load to the rubber-soil mixture to assess its mechanical response. The testing consisted of compacting a layer of rubber-soil mixture and applying a load above the sample. The primary parameters considered were the magnitude of the applied loads and soil sample types. The performance of the backfill material was further assessed by examining the relationship between the applied load and the resulting horizontal displacement of the retaining wall model.

2.2.3 Kenaf fibre-soil reinforced block properties tests

The kenaf fibres underwent an alkaline chemical treatment to enhance their mechanical performance and interfacial bonding with the soil matrix. The fibres were soaked in sodium hydroxide (NaOH) solutions at varying concentrations for 1 and 3 hours, then thoroughly washed with distilled water to remove residual chemicals. The treated fibres were oven-dried at 80°C for 24 hours to remove residual moisture. Soil reinforced with kenaf fibres was prepared using the optimum fibre content determined from preliminary mechanical property tests. The reinforced soil mixture was subsequently placed in a mould and compacted using a table compactor machine and tamping to achieve uniform density. In accordance with ASTM D1632 [28], the moulded blocks were cured under controlled temperature and humidity conditions for 7 to 28 days to ensure adequate strength development and durability. The procedure, which involved controlled mixing, mechanical compaction and standard curing, ensured the production of durable kenaf fibre-reinforced soil blocks suitable for construction applications. A representative kenaf fibre–soil reinforced block specimen is shown in Figure 4. Following the fabrication of soil-reinforced blocks, compressive strength tests were conducted to assess their load- bearing capacity. The blocks were tested using a universal testing machine, in which a progressive compressive load was applied until failure. The compressive strength tests were performed in accordance with ASTM C109/C109M [29], which specifies procedures for determining the compressive strength of cylindrical concrete specimens. In addition, flexural strength tests were conducted to assess the bending performance of the soil-reinforced blocks. These tests were carried out in accordance with the guidelines of ASTM D1635/D1635M [30], which are used to determine the flexural strength of soil–cement mixtures. During the test, each soil-reinforced block was placed on a support span, and a load was applied at the mid-span until cracking occurred. The flexural strength was calculated based on the recorded fracture load, block dimensions, and span length.

Figure 4. Sample of kenaf fiber - soil reinforced block

2.2.4 Advanced retaining system monitoring using IoT sensors

An IoT-based monitoring system was developed by integrating multiple sensors to provide real-time data on critical parameters affecting the performance of retaining walls. The system consists of three primary layers: the sensing layer, comprising distributed sensor nodes; the communication layer, utilising an ESP32 microcontroller with built-in Wi-Fi; and the data visualisation and analysis layer, implemented via the Blynk IoT platform. This multi-layered design ensures robust data gathering, transmission and processing capabilities essential for continuous slope monitoring applications [31]. In the slope model, soil moisture sensors were placed in two critical locations, uphill and downhill, and were connected to the analogue pins 35 and 34 on the ESP32 microcontroller. The soil moisture sensors used capacitive sensing technology, which provides higher precision and longer-term stability. These sensors were calibrated using the gravimetric method to establish a correlation between volumetric water content and sensor output voltage, ensuring measurement accuracy across the operational range. These sensors allowed continuous monitoring of soil moisture content over a range of 0-100%, enabling detection of saturation levels that can influence slope stability. Moreover, temperature and humidity measurements were obtained using DHT22 sensors connected to digital pin 33 of the ESP32 microcontroller.

Temperature sensors help monitor the soil's ambient temperature, as temperature changes can affect soil characteristics and shear strength. Temperature variations affect pore-water pressure dynamics and soil viscosity, which in turn influence the effective stress and shear strength parameters critical to slope stability analysis. In addition, humidity sensors monitor soil moisture, as it affects soil cohesion and shear strength, which can lead to landslides. Finally, tilt sensors were incorporated to monitor the retaining wall's inclination. The tilt sensors utilised MEMS (Micro-Electro-Mechanical Systems) accelerometer technology capable of detecting angular displacements with 0.1° resolution. The sensors were configured to trigger alerts when inclination changes exceeded predefined thresholds, enabling proactive intervention before critical failure conditions develop [32]. Continuous tracking of wall angles enabled early detection of potential tilting or structural instability. The integration of multiple sensor types allowed comprehensive monitoring of environmental and structural parameters, providing essential data for early warning and slope stability assessment (see Figure 5). The testing procedure used predetermined water volumes of 1000, 3000, and 5000 ml applied over durations of 20, 40, and 60 seconds to simulate controlled rainfall. This systematic approach enabled a thorough evaluation of the system's performance across various rainfall durations and intensities that reflect natural weather conditions. Important indicators of slope stability and retaining wall performance were the monitoring results during rainfall simulation.

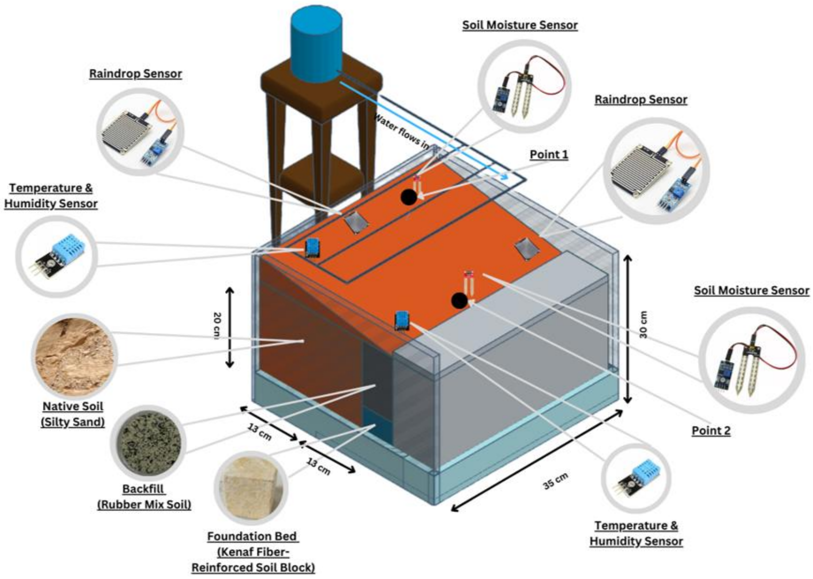

Figure 5. Sensor placement on retaining wall with crumb rubber-soil backfill and kenaf fiber-reinforced soil blocks

Figure 6. Real time monitoring on sensors using Blynk applied on the advanced retaining system

Continuous monitoring using IoT platforms like Blynk, as shown in Figure 6, can provide real-time data, enabling early warning systems to mitigate risks associated with soil saturation and landslides. The Blynk platform facilitates data logging at user-defined intervals (configured at a 5-minute sampling rate in this study), cloud-based data storage, and customizable alert notifications when parameter thresholds are exceeded. The system's wireless connectivity eliminates the need for hardwired data acquisition systems, significantly reducing installation complexity and enabling deployment in remote or difficult-to-access locations. This real-time approach is crucial for effective risk management in areas with heavy rainfall and steep terrains.

2.2.6 Finite element modelling of retaining wall system

A two-dimensional finite element analysis was conducted using PLAXIS 2D to evaluate the stability and deformation behaviour of the proposed retaining wall system. PLAXIS 2D was selected for this analysis due to its proven capabilities in geotechnical analysis and widespread validation in retaining wall applications. The software employs advanced numerical algorithms specifically optimised for soil-structure interaction problems and provides robust constitutive models for various soil types [33]. PLAXIS 2D has been thoroughly tested against field measurements and analytical solutions for retaining wall systems, demonstrating greater accuracy than conventional limit equilibrium methods in predicting lateral displacements and stress distributions [34]. PLAXIS 2D was effectively employed to analyse the seismic behaviour of retaining structures, which demonstrates its accuracy under dynamic loading conditions [35]. Additionally, the software was particularly suitable for analysing innovative retaining wall systems that use non-conventional materials because of its capacity to replicate complex loading conditions, groundwater movement, and staged construction sequences. The automatic mesh generation and optimisation algorithms in PLAXIS 2D minimise computational demands while ensuring numerical stability, thereby enabling parametric studies that are crucial for design optimisation. The model geometry was developed with dimensions of a 3 m high retaining wall with a 2 m width, incorporating rubber-soil backfill and kenaf fibre-reinforced soil block as a foundation bed (Figure 7). Figure 8 shows the deformed mesh of the retaining wall system, generated prior to the plastic analysis and safety factor calculation. The modelling of rubber-soil backfills and kenaf fibre-reinforced soil blocks was performed using this software, which required shear strength parameters such as the internal friction angle and cohesion. The Mohr-Coulomb constitutive model was adopted for all soil materials, with material parameters assigned based on laboratory test results from Phase 1 and Phase 2 of the experimental program.

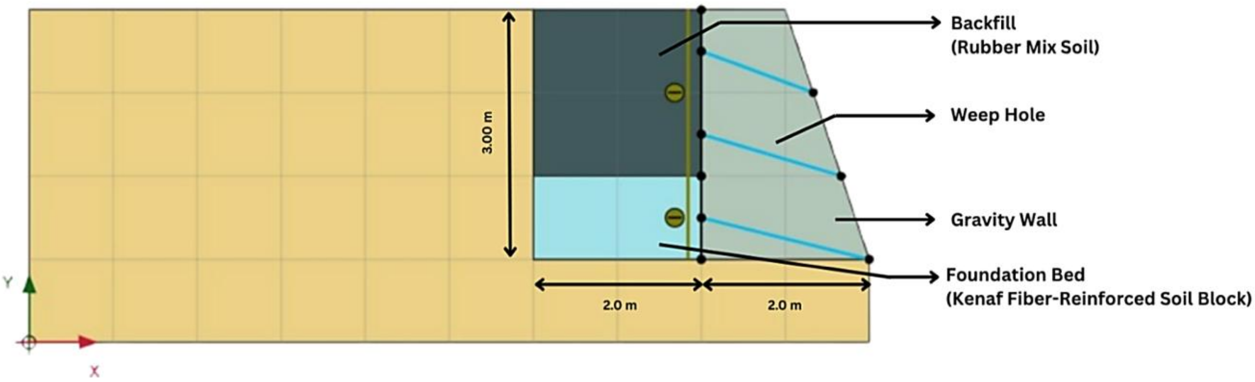

Figure 7. Retaining wall system in Plaxis 2D

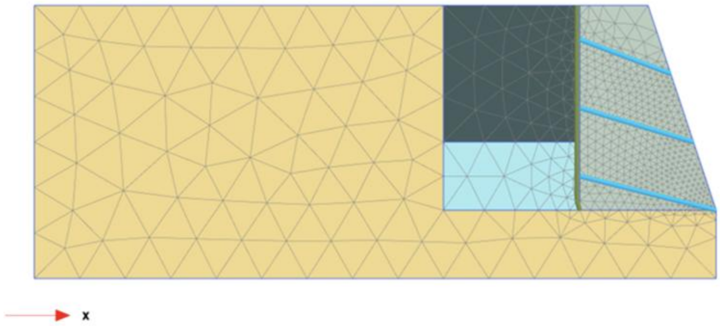

Figure 8. Deformed mesh of retaining wall system in Plaxis 2D

3. Results And Discussion

3.1 Geotechnical Properties of Soil Sample

The physical properties and mechanical properties of the studied soil sample were tabulated in Table 1. Table 1 presents particle size distribution parameters, specific gravity values, soil characteristics, Atterberg limits defining plasticity behaviour, shear strength parameters obtained from direct shear testing, standard proctor compaction characteristics, and permeability coefficients indicating low hydraulic conductivity. These parameters act as a baseline soil property essential for evaluating the effectiveness of kenaf fibre reinforcement and rubber-soil properties backfill improvements. The studied soil sample was predominantly sand (77.1%), with a significant percentage of fine particles (22.7%) and a negligible amount of gravel (0.2%) (Table 1). Increased fines content may reduce permeability, leading to water retention issues and gradual deterioration of soil structure [36]. The specific gravity was reported at 2.79. This value indicates a denser soil composition. The Atterberg limit values showed that a liquid limit (LL) of 44.74%, plastic limit (PL) of 34.03% and plasticity index (PI) of 10.71%, which falls below the A-line on the plasticity chart, indicated low silt content – ML, as shown in Figure 9 (based on Unified Soil Classification System - USCS). Thus, based on the particle-size distribution and Atterberg limit analysis, the soil sample studied can be classified as Silty Sand (SM) under the Unified Soil Classification System (USCS).

Table 1. Geotechnical properties values of the studied soil sample

Properties	Unit	Values
Grain Size Distribution		
- Gravel	%	0.20
- Sand	%	77.1
- Fines (Clay, Silt)	%	22.7
*USCS	-	*SM
Specific Gravity, G_s	-	2.79
Plastic Limit, PL	%	34.0
Liquid Limit, LL	%	44.7
Plasticity Index, PI	%	10.7
Linear Shrinkage Limit, LS	%	2.1
Optimum Moisture Content, OMC	%	15
Maximum Dry Density, MDD	kg/m^3	1640
Cohesion, *c*	kPa	12.16
Internal Friction Angle, ϕ	°	18.63
Permeability, *k*	m/s	4.47 x 10^{-5}

Notes: USCS – Unified Soil Classification System; SM – Silty Sand

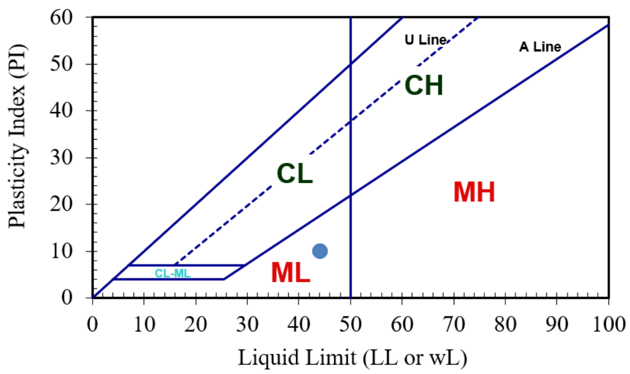

Figure 9. Plasticity index value of the studied soil sample on the chart

The soil achieved its maximum dry density of 1640 kg/m³ at an optimum moisture content of 15% (Table 1). The typical values reported for SM-classified soils in tropical climates align well with these compaction parameters, which are characteristics of silty sand soils [37]. The influence of fines content, which requires more water to provide lubrication between particles during compaction, was shown in relatively high optimum moisture content [38]. The presence of fine particles, particularly silt, in the studied soil sample influenced its response to compaction by affecting particle rearrangement and moisture retention. The shear strength parameters obtained from the direct shear test indicated an internal friction angle of 18.63° and a cohesion value of 12.16 kPa. These values characterise the soil as having a low frictional strength and moderate cohesion. The moderate cohesion of 12.16 kPa results from apparent cohesion due to capillary forces and the binding effect of silt particles [39]. Consequently, the soil exhibits intermediate shear-strength behaviour, necessitating careful geotechnical design considerations for slopes, foundations, and retaining structures due to its limited frictional resistance and moderate cohesive contribution. The permeability coefficient of the studied soil sample was 4.47×10^{-5} m/s, indicating low permeability. Although not as impermeable as clay, the permeability range is typically associated with fine-grained soils such as silts and clays. Such soils exhibit restricted water flow, which may result in poor drainage characteristics and increased susceptibility to water retention.

3.2 Crumb Rubber Tire Waste-Soil Backfill Material Analysis

The combined effect of cohesion and angle of friction is crucial in the design of retaining walls, as soil parameters are used in various earth pressure theories to determine lateral earth pressure and calculate the total force acting on the wall. Table 2 presents a comprehensive comparison of the geotechnical parameters for the natural soil and soil mixed with varying percentages of tyre waste, demonstrating the systematic evaluation conducted to identify the optimal rubber content. According to Table 2, the control sample exhibited baseline properties with moderate cohesion (12.16 kPa) and internal friction angle (18.63°), along with a permeability of 4.47×10^{-5} m/s, typical of silty sand. At 10% rubber content, the internal friction angle increased to 21.11° while cohesion decreased slightly to 11.63 kPa, indicating enhanced particle interlocking and frictional resistance. This behaviour is consistent with previous studies demonstrating that the initial addition of rubber improves frictional properties by enhancing particle interlocking and surface roughness [40]. This improvement continued at a 20% rubber concentration, achieving the optimum percentage, with cohesion increasing to 17.96 kPa and an internal friction angle of 19.64°. Optimal tyre chip content was found between 15-25% for sand-tire mixtures, which demonstrated maximum shear strength improvements in this range [40]. The enhanced cohesion at this concentration can be attributed to the elastic nature of rubber particles, which create a more integrated soil-rubber matrix that better distributes stresses and provides improved resistance to shear deformation. The 47.7% increase in cohesion at 20% rubber content represents a significant improvement that directly translates to enhanced backfill performance. The compressible rubber particles undergo elastic deformation under shear loading, thereby distributing stresses more uniformly throughout the soil matrix and avoiding stress concentrations at particle contacts [42]. However, at 30% and 40%, cohesion increased to 27.62 kPa and then decreased to 24.12 kPa, respectively, while friction angles showed inconsistent behaviour, suggesting that excessive rubber content may disrupt the soil structure and reduce the efficiency of particle interaction.

Table 2. Crumb rubber tyre waste-soil mixture properties for backfill material selection

Rubber content (%)	Cohesion, c (kPa)	Internal friction angle, φ (°)	Permeability, k ($\times 10^{-5}$ m/s)
0 (Control)	12.16	18.63	4.47
10	11.63	21.11	4.13
20	17.96	19.64	4.20
30	27.62	17.17	5.65
40	24.12	19.32	6.50

Table 3. Summary of total active force acting on wall

Sample	Unit weight, γ (kN/m^3)	Coefficient of Active Pressure, Ka	Total active force = Pa + Ps (kN)
Natural soil	1.399	0.154	0.187
Soil + 20% tires waste	1.549	0.155	0.207

Table 3 presents the calculation of the total active force on the retaining wall for the natural soil and the soil mixed with 20% tyre waste. Active earth pressure refers to the lateral pressure exerted by the backfill soil on the retaining wall, which tends to cause outward movement of the wall [43]. This pressure is typically the dominant force acting on the retaining wall and is influenced by soil properties, the wall geometry, and surcharge loading conditions. The total active force for natural soil was 0.187 kN, derived from a unit weight of 1.399 kN/m³ and a coefficient of active pressure (Ka) of 0.154. The soil-rubber mixture with 20% tyre waste demonstrated an increase in the total active force to 0.207 kN, corresponding to a unit weight of 1.549 kN/m³ and Ka of 0.155. This 10.7% increase in active force requires careful consideration in the context of retaining wall design and performance. The increase in active earth pressure observed with 20% rubber content must be evaluated within the broader framework of retaining wall stability and performance. While higher active forces initially appear to impose greater loading demands on the retaining structure, this increase is accompanied by several compensating improvements in the backfill material properties that enhance overall system performance.

Tire-derived aggregate (TDA) provides greater long-term performance through improved drainage, reduced settlement and enhanced resistance to freeze-thaw cycles, even though its higher unit weight slightly increases the lateral earth pressure coefficient [44]. In full-scale field tests, retaining walls with tyre chip backfill exhibited reduced lateral movement even though active forces were theoretically increased, which is attributed to the compressible nature of rubber particles, which accommodate deformation without producing high stress concentrations [45]. The enhanced cohesion of 17.96 kPa, compared to 12.16 kPa for natural soil, and the maintained friction angle of 19.64°, compared to 18.63°, indicate that the rubber-soil mixture provides superior shear resistance, which is critical for preventing internal failure within the backfill mass itself. The improved mechanical properties suggest that the backfill material can better resist internal deformation and maintain its structural integrity under loading conditions. Furthermore, the elastic properties of rubber particles confer beneficial compressibility that improves stress distribution and reduces stress concentrations at the wall-backfill interface. Tire chips incorporated in backfill materials significantly lowered seismic earth pressures by absorbing vibration energy, improving performance during earthquake loading [46]. The lightweight nature of rubber, compared with conventional aggregate, also reduces the total dead load on foundation systems, potentially enabling more cost-effective foundation designs [47]. The slight increase in active force is therefore offset by improved load distribution mechanisms that enhance the long-term performance and durability of the retaining system.

3.3 Behaviour of Kenaf Fiber- Soil Reinforced Blocks

The strength properties of kenaf fibre-reinforced soil blocks, namely compressive and flexural strength, are shown in Figure 10. The soil blocks using natural soil have a compressive strength of 0.75 N/mm². Adding 0.75% treated kenaf fibre by weight of soil results in a compressive strength of 0.96 N/mm², which is higher than that of the natural soil. Figure 10 also demonstrates that the addition of kenaf fibre significantly enhances the compressive strength of soil blocks, as this fibre is more effective in them. The improved compressive strength can be attributed to the fibres' capacity to enhance load distribution within the soil matrix and to hinder crack propagation under compressive loads [48]. This bonding improves the overall structural integrity and load-bearing capacity of the soil block. Additional research has supported similar findings, demonstrating that natural fibres can significantly enhance the mechanical properties of soil-reinforced blocks, making them suitable for a range of building applications [49]. Furthermore, it is also shown that the flexural strength of the natural soil and soil with 0.75% treated kenaf fibre. The soil blocks with natural soil indicate a flexural strength of 0.64 N/mm². When comparing the samples, the sample containing 0.75% treated kenaf fibre exhibits a higher flexural strength of 0.75 N/mm². The results suggest that the inclusion of natural fibres improves the bending resistance of soil-reinforced blocks. These characteristics enable the fibres to distribute stresses more uniformly within the block, thereby enhancing its overall strength [50].

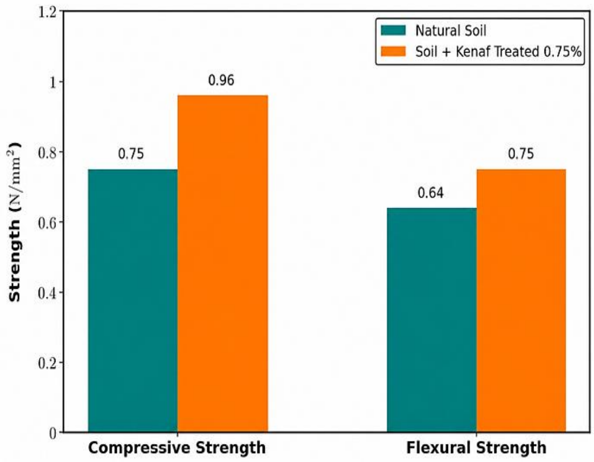

Figure 10. Compressive strength and flexural strength values of soil and kenaf-reinforced soil blocks

3.4 Advanced Retaining System Monitoring using IoT Sensors

The analysis of soil moisture readings and runoff data provides significant insights into soil behaviour under varying water application conditions. These parameters provided detailed views of changes in water infiltration and runoff under different volumes and durations. Table 4 presents water runoff and infiltration at water application volumes of 1000 ml, 3000 ml, and 5000 ml, with durations of 20, 40, and 60 seconds. The data show that water runoff increases with the volume of water applied, with a significant portion of the water infiltrating the soil at higher volumes and longer durations (Table 4). At smaller water volumes and durations, infiltration was low, and most of the water contributed to runoff, whereas at higher volumes and durations, infiltration and runoff were more balanced. The infiltration theory explains that the soil initially absorbs water quickly due to high matric suction, but as pore spaces become saturated, the infiltration rate decreases and approaches the soil's steady-state hydraulic conductivity [51]. These results show the soil's potential for absorption and the need for proper water management, underscoring the importance of understanding soil moisture and runoff dynamics, particularly in regions susceptible to rainfall-induced landslides.

The slope angle remains relatively stable at a lower volume of 1000 ml across all durations (20, 40, and 60 seconds), as indicated in Figure 11. Specifically, the slope angle remains constant at 45.0° before and after the simulation at 20 seconds. This stability is maintained with only a slight movement to 44.8° after 60 seconds. These results demonstrate the soil integrity at lower moisture levels. In contrast, the slope angle changes significantly when the water volume increases to 3000 ml and 5000 ml, indicating increased soil moisture and infiltration. The slope angle was shown to drop to 44.9° at 20 seconds, 44.7° at 40 seconds, and decrease to 44.5° after 60 seconds for 5000 ml. The 0.5° reduction corresponds to a change in slope angle of about 1.1%, which might seem minor but can have significant implications for slope stability [52]. Predictable patterns in the literature on soil mechanics show that when water penetrates the soil, it can increase pore water pressures, reducing effective stress and shear strength [53]. This indicates deeper infiltration and more substantial water absorption. At 3000 ml, the slope angle dropped to 44.9° after 40 seconds and 44.8° after 60 seconds (Figure 11). This implies that higher water volumes will cause the soil to become more saturated, which can alter soil stability. This behaviour showed that the slope angle, runoff volume, and soil moisture provide information about soil behaviour across various scenarios. Higher water volumes lead to greater infiltration and reduced stability.

Table 4. Summary of volume of water, water runoff and water infiltration varied by rainfall duration

Rainfall Duration (s)	Volume of Water (ml)	Water Runoff (ml)	Water Infiltration (ml)
20	1000	900	100
	3000	2500	500
	5000	4200	800
40	1000	730	270
	3000	2100	900
	5000	3300	1700
60	1000	600	400
	3000	1600	1400
	5000	2100	2900

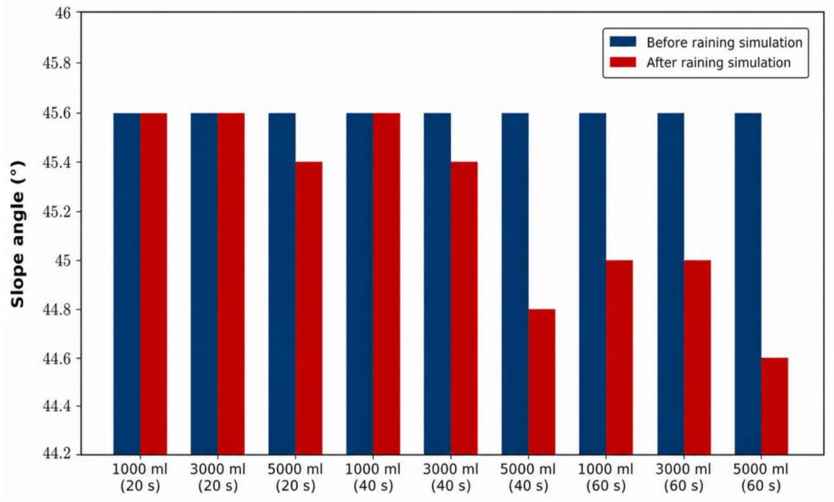

Figure 11. Impact of variation in precipitation on variation of slope angle

3.5 Software Analysis (Plaxis2D) of Retaining Wall System

The finite element analysis results demonstrated significant performance differences between the retaining wall system using natural soil and the retaining wall system using combined kenaf fibre soil-reinforced block-rubber soil backfill. The displacement contours revealed that the retaining wall system using natural soil exhibited a maximum displacement of 5.008×10^{-3} m (5.0 mm) occurring at the upper portion of the retaining wall near Element 517, Node 661 (Figure 12). The displacement distribution showed characteristic patterns with maximum values concentrated at the wall crest and gradually decreasing toward the base, consistent with typical cantilever retaining wall behaviour under lateral earth pressure. Numerous theoretical and experimental investigations on the behaviour of retaining walls have validated that this displacement pattern is consistent with the theory of classical soil mechanics [54]] – [[55]. In contrast, the combined retaining wall system demonstrated a maximum displacement of only 1.320×10^{-3} m (1.3 mm) at Element 1, Node 3913, representing a remarkable 73.6% reduction compared to the natural soil configuration (Figure 13). The displacement contours in the combined retaining wall systems showed a more uniform distribution and substantially smaller magnitudes throughout the structure, indicating enhanced load transfer mechanisms and improved stress distribution, attributed to the superior mechanical properties of both the rubber-soil backfill and the kenaf fibre-reinforced soil blocks.

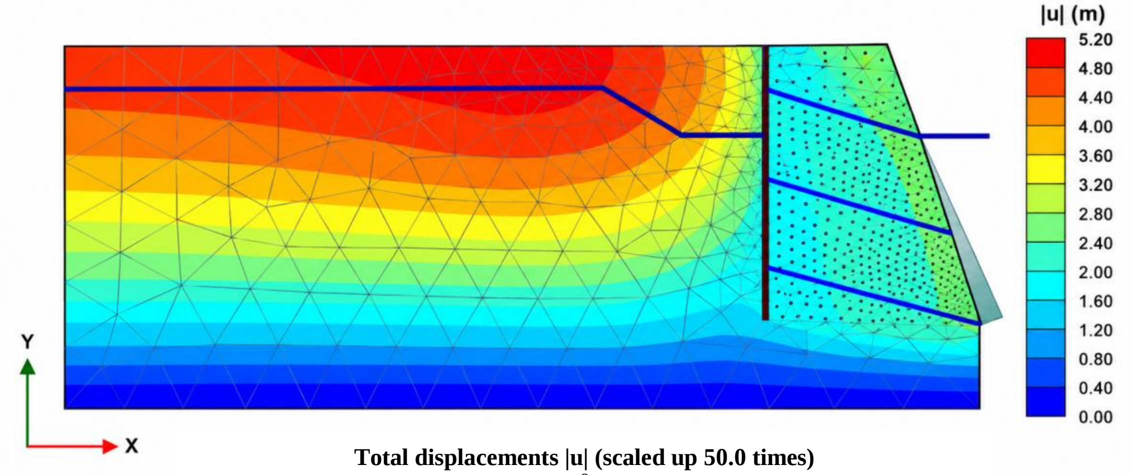

Total displacements |u| (scaled up 50.0 times)
Maximum value = 5.008×10^{-3} m (Element 517 at Node 661)

Figure 12. Total displacements result of retaining wall system using natural soil

The numerical validation through PLAXIS 2D modelling provides strong technical evidence supporting the viability of the proposed combined retaining wall system for practical applications. The significant reduction of 73.6% in lateral displacement offers significant advantages for structures with strict serviceability requirements where excessive movement could cause functional problems or damage to adjacent infrastructure. The stress distribution patterns revealed that the retaining wall system using natural soil exhibited higher stress concentrations at the wall base characteristic of passive failure zones, whereas the combined retaining wall system showed more uniform stress distribution with deeper potential failure surfaces extending into the foundation soil, indicating better mobilisation of backfill strength and reduced vulnerability to surface instabilities. Furthermore, beneath the retaining wall, the kenaf-fibre-reinforced foundation soil exhibited exceptional stability and bearing capacity with minimal deformation. By increasing shear strength, ductility, and resistance to strain localisation, the inclusion of kenaf fibre enhances the engineering behaviour of soil, particularly in sand–clay mixes. This is consistent with the results from extensive direct shear tests showing that kenaf fibre reinforcement improves post-peak behaviour and boosts shear strength, thereby lowering the risk of abrupt failure and settlement [12]. The simulation, in which the wall remained upright and base motion was minimal, validated this behaviour. This is consistent with the minimal deformation seen in the base zone, demonstrating the material's effective stress distribution under the backfill load and the wall's self-weight. Lateral drainage was made possible by the weep holes drilled through the wall, which significantly reduced hydrostatic accumulation behind the wall by dissipating pore water pressure during the flow analysis phase. From both technical and environmental perspectives, the combined retaining wall system demonstrates superior performance by incorporating waste tyre rubber and renewable kenaf fibres into the soil, aligning with sustainable construction principles.

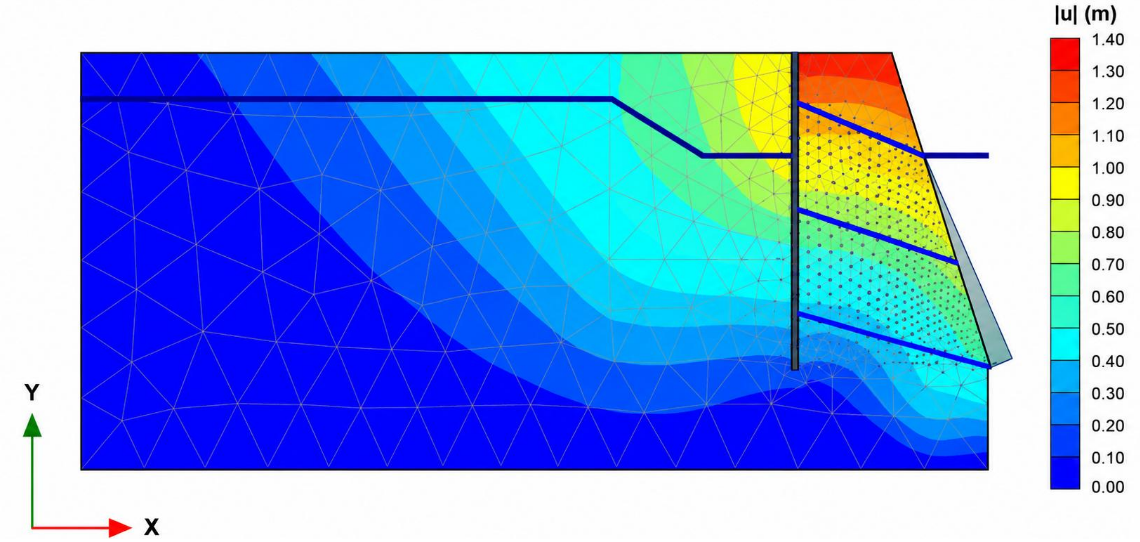

Total displacements |u| (scaled up 200 times)
Maximum value = 1.320 × 10^{-3} m (Element 1 at Node 3913)

Figure 13. Total displacements result of retaining wall system using combined kenaf fiber soil reinforced block-rubber soil backfills

The proposed advanced retaining wall system demonstrates measurable performance advantages compared to conventional retaining wall technologies across multiple evaluation criteria. Conventional retaining walls utilising natural granular backfill typically exhibit lateral displacements in the range of 5-8 mm under comparable loading conditions and geometry, whereas the current system achieved only 1.3 mm displacement. This performance is superior to that of conventional geogrid-reinforced soil retaining walls, which typically achieve lateral displacement reductions of 30-40% compared to unreinforced systems [56]. Additionally, economic research indicates that the proposed system offers significant cost advantages where kenaf fibres are low-carbon, renewable substitutes for energy-intensive cement manufacturing [57], and waste tyre rubber is often available at minimal or negative cost due to disposal fees [58]. The synergistic combination of several enhancement mechanisms operating simultaneously is responsible for the superior performance of the proposed system which were the elastic compressibility of rubber particles that distributes stresses more evenly than rigid reinforcement elements, the three-dimensional fibre reinforcement in the foundation blocks that provides enhances isotropic strength in contrast to uniaxial geogrid reinforcement and the improved cohesion in the rubber-soil backfill which lowers active earth pressure more effectively than friction only improvements.

4. Conclusions

This study demonstrates the feasibility and advantages of an innovative smart retaining wall system integrating kenaf fibre-reinforced soil blocks, rubber-soil backfill and an IoT-based real-time monitoring framework at laboratory scale. The kenaf fibre with 0.75% fibre concentration was shown to significantly improve mechanical strength; moreover, the rubber-soil mixture, as a backfill material, enhanced geotechnical properties such as friction angle and cohesion. The evaluation across five rubber concentrations (0%, 10%, 20%, 30%, 40%) identified 20% as optimal through multi-criteria analysis balancing cohesion enhancement, friction angle stability, and physical model performance. While rubber inclusion slightly increased active earth pressure by 10.7%, this was more than offset by enhanced backfill cohesion with a 47.7% increase, improved stress distribution, and the superior load-bearing capacity of kenaf fibre-reinforced soil blocks, resulting in a net 73.6% reduction in system-level lateral displacement compared to conventional natural soil systems. This displacement reduction substantially exceeds performance improvements reported for conventional geogrid-reinforced systems (30-40%), demonstrating the superior effectiveness of the synergistic combination of elastic rubber particles and three-dimensional fibre reinforcement. Although the inclusion of rubber waste increased the active earth pressure, the retaining wall system remained structurally stable when properly designed. Furthermore, the IoT monitoring system effectively captured critical environmental variables, providing real-time data for early detection of slope conditions susceptible to landslides. The laboratory-scale findings establish strong baseline performance characteristics and validate the conceptual framework of synergistic integration between sustainable waste materials and intelligent monitoring systems.

Acknowledgements
The authors express their sincere gratitude to the Department of Civil Engineering and the Faculty of Engineering at Universiti Putra Malaysia, Malaysia, as well as the staff members that helped them finish the works.

Funding
This study was supported and funded by Universiti Putra Malaysia (Project Code: GP-IPS/2021/9701400, Grant Type: Geran Inisiatif Putra Siswazah (GP-IPS) is highly appreciated.

Declaration of Competing Interest
The author declares no conflicts of interest.

Credit Authorship Contribution Statement
Zaffri Zaki (Methodology development; Formal analysis; Writing - original draft; Writing - review & editing)
Nik Norsyahariati Nik Daud (Conceptualization; Supervision; Project administration; Resources)
Muhammad Zulhafizi Muhammad Zuraidi (Methodology development; Formal analysis; Writing - original draft; Writing - review & editing)
Abdullah Iman Sahatim (Methodology development; Formal analysis; Writing - original draft; Writing - review & editing)
Abubakar Sadiq Muhammed (Writing - review & editing)

Availability of Data and Materials
The data supporting this study's findings are available on request from the corresponding author.

Ethics Declarations
This study did not involve human participants or animals. Ethical approval was therefore not required.

Generative Artificial Intelligence Declarations
The authors claim that artificially intelligent-assisted technologies, such as generative AI, were not used to generate content, ideas, or theories. We have just utilised AI to enhance readability and refine the language. This was used with extreme human control and oversight. The authors take full responsibility for reviewing and approving the content.

References
[1] K.G. Garg, "Retaining wall with reinforced backfill – a case study," *Geotextiles and Geomembranes*, vol. 16, no. 3, pp. 135–149, 1998, https://doi.org/10.1016/S0266-1144(98)00003-X.
[2] S.B. Reddy, and A.M. Krishna, "Recycled tire chips mixed with sand as lightweight backfill material in retaining wall applications: an experimental investigation," *International Journal of Geosynthetics and Ground Engineering*, vol. 1, no. 4, pp. 1–11, 2015, https://doi.org/10.1007/s40891-015-0036-0.
[3] M. Akbar, P. Huali, J. Huang, et al., "Seismic response comparison of various geogrid reinforced earth-retaining walls: based on shaking table and 3D FE analysis," *Scientific Reports*, vol. 14, no. 1, pp. 1–23, 2024, https://doi.org/10.1038/s41598-024-64203-4.
[4] V. Cecich, L. Gonzales, A. Hoisaeter, J. Williams, and K. Reddy, "Use of shredded tires as lightweight backfill material for retaining structures," *Waste Management & Research*, vol. 14, no. 5, pp. 433–451, 1996, https://doi.org/10.1177/0734242X9601400503.
[5] S.M.B. Helwany, G. Reardon, and J.T.H. Wu, "Effects of backfill on the performance of GRS retaining walls," *Geotextiles and Geomembranes*, vol. 17, no. 1, pp. 1–16, 1999, https://doi.org/10.1016/S0266-1144(98)00021-1.
[6] N.F. Isa, M.F.M. Zaki, L.A. Sofri, M.A. Rahim, Z.M. Ghazaly, and N. Bidin, "The use of rubber manufacturing waste as concrete additive," *Journal of Advances in Applied Mechanics*, vol. 4, no. 1, pp. 12–18, 2014.
[7] B. Indraratna, S. Nimbalkar, and T. Neville, "Performance assessment of reinforced ballasted rail track," *Proceedings of the Institution of Civil Engineers - Ground Improvement*, vol. 167, no. 1, pp. 24–34, 2014, https://doi.org/10.1680/grim.13.00018.
[8] H. Cetin, M. Fener, and O. Gunaydin, "Geotechnical properties of tire-cohesive clayey soil mixtures as a fill material," *Engineering Geology*, vol. 88, no. 1, pp. 110–120, 2006, https://doi.org/10.1016/j.enggeo.2006.09.002.
[9] S. Akbulut, S. Arasan, and E. Kalkan, "Modification of clayey soils using scrap tire rubber and synthetic fibers," *Applied Clay Science*, vol. 38, no. 1, pp. 23–32, 2007, https://doi.org/10.1016/j.clay.2007.02.001.
[10] T. Zafar, M.A. Ansari, and A. Husain, "Soil stabilization by reinforcing natural and synthetic fibers – A state of the art review," *Materials Today: Proceedings*, early access, 2023, https://doi.org/10.1016/j.matpr.2023.03.503.
[11] A.A. Mohamad Mazuki, H. Md Akil, S. Safiee, Z. Ishak, and A. Bakar, "Degradation of dynamic mechanical properties of pultruded kenaf fiber reinforced composites after immersion in various solutions," *Composites Part B: Engineering*, vol. 42, pp. 71–76, 2011, https://doi.org/10.1016/j.compositesb.2010.08.004.
[12] N. Esmaeilpour Shirvani, A. Taghavi Ghalesari, M. Khaleghnejad Tabari, and A.Janalizadeh Choobbasti, "Improvement of the engineering behavior of sand-clay mixtures using kenaf fiber reinforcement," *Transportation Geotechnics*, vol. 19, pp. 1–8, 2019, https://doi.org/10.1016/j.trgeo.2019.01.004.

[13] R. Munirwan, M. Munirwansyah, M. Marwan, R. Putra Jaya, and V. Kamchoom, “Performance of coir fiber addition for clay as a sub-grade for pavement design,” in *IOP Conference Series: Materials Science and Engineering*, vol. 712, p. 012009, pp. 1–8, 2020, https://doi.org/10.1088/1757-899X/712/1/012009.
[14] M.U. Maguesvari, P. Muthaiyan, and S. Yugasini, “Stabilization of soil using kenaf fibre and rice husk ash,” *Materials Today: Proceedings*, 2023, https://doi.org/10.1016/j.matpr.2023.06.261.
[15] R. Abbasov, M. Fahs, A. Younes, H. Nowamooz, K. Jørgen Måløy, and R. Toussaint, “Modeling rainfall-induced landslide using the concept of local factor of safety: Uncertainty propagation and sensitivity analysis,” *Computers and Geotechnics*, vol. 167, p. 106102, pp. 1–22, 2024, https://doi.org/10.1016/j.compgeo.2024.106102.
[16] X. Liu, and Y. Wang, “Quantifying impacts of precipitation scenarios projected under climate change on annual probability of rainfall-induced landslides at a specific slope,” *Computers and Geotechnics*, vol. 167, p. 106063, pp. 1–19, 2024, https://doi.org/10.1016/j.compgeo.2023.106063.
[17] Y. Lee, W.-H. Choi, and S.-C. Kim, “Slope monitoring system for nuclear power plants,” *Nuclear Engineering and Design*, vol. 347, pp. 86–94, 2019, https://doi.org/10.1016/j.nucengdes.2019.03.019.
[18] H. Dou, R. Wang, H. Wang, and W. Jian, “Rainfall early warning threshold and its spatial distribution of rainfall-induced landslides in China,” *Rock Mechanics Bulletin*, vol. 2, no. 3, pp. 1–13 2023, https://doi.org/10.1016/j.rockmb.2023.100056.
[19] W-H. Zhou, X. Xu, and A. Garg, “Measurement of unsaturated shear strength parameters of silty sand and its correlation with unconfined compressive strength,” *Measurement*, vol. 93, pp. 351–358, 2016, https://doi.org/10.1016/j.measurement.2016.07.049.
[20] S.M. Karunarathne, M. Dray, L. Popov, M. Butler, C. Pennington, and C.M. Angelopoulos, “A technological framework for data-driven IoT systems: Application on landslide monitoring,” *Computer Communications*, vol. 154, pp. 298–312, 2020, https://doi.org/10.1016/j.comcom.2020.02.076.
[21] Geological Survey of Peninsular Malaysia (MyGEMS), “ Geological Map of Peninsular Malaysia,” Minerals and Geoscience Department Malaysia, 2025. [Online]. Available: https://mygems.jmg.gov.my/portal/apps/sites/#/mygems-awam/
[22] ASTM D6913-04, Standard test methods for particle-size distribution (gradation) of soils using sieve analysis. West Conshohocken, PA, USA: International, 2007. https://doi.org/10.1520/D6913-04R09E01.
[23] ASTM D4318-17, Standard test methods for liquid limit, plastic limit, and plasticity index of soils. West Conshohocken, PA, USA: International, 2017. https://doi.org/10.1520/D4318-17.
[24] ASTM D854-14, Standard test methods for specific gravity of soil solids by water pycnometer. West Conshohocken, PA, USA: International, 2014. https://doi.org/10.1520/D0854-14.
[25] ASTM D698-12(2021) , Standard test methods for laboratory compaction characteristics of soil using standard effort (12,400 ft-lbf/ft3 (600 kn-m/m3)). West Conshohocken, PA, USA: International, 2021. https://doi.org/10.1520/D0698-12R21.
[26] ASTM D3080-04, Standard test method for direct shear test of soils under consolidated drained conditions. West Conshohocken, PA, USA: International, 2004. https://doi.org/10.1520/D3080-04.
[27] ASTM D5084-03, Standard test methods for measurement of hydraulic conductivity of saturated porous materials using a flexible wall permeameter. West Conshohocken, PA, USA: International, 2003. https://doi.org/10.1520/D5084-03.
[28] ASTM D1632-17, Standard practice for making and curing soil-cement compression and flexure test specimens in the laboratory. West Conshohocken, PA, USA: International, 2017. https://doi.org/10.1520/D1632-17.
[29] ASTM C109/C109M-20, Standard test method for compressive strength of hydraulic cement mortars (using 2-in. or [50-mm] cube specimens). West Conshohocken, PA, USA: International, 2020. https://doi.org/10.1520/C0109_C0109M-20.
[30] ASTM D1635/D1635M-19, Standard test method for flexural strength of soil-cement using simple beam with third-point loading. West Conshohocken, PA, USA: International, 2019. https://doi.org/10.1520/D1635_D1635M-19.
[31] D. Devasena, R. Ramya, D. Yuvaraj, S. Vivek, and T. Darshan, “IoT based water distribution system,” *International Journal of Engineering and Advanced Technology*, vol. 8, no. 6, pp. 132–135, 2019, https://doi.org/10.35940/ijeat.D6295.088619.
[32] H. Xu, F. Li, Y. Gao, and W. Wang, “Simultaneous measurement of tilt and acceleration based on FBG sensor,” *IEEE Sensors Journal*, vol. 20, no. 24, pp. 14857–14864, 2020, https://doi.org/10.1109/JSEN.2020.3010851.
[33] R. Brinkgreve, WM. Swolfs, E. Engin, *et al.*, “PLAXIS 2D Reference manual,” *Delft University of Technology and PLAXIS bv the Netherlands*, 2011.
[34] D.M. Potts, and L. Zdravkovic, *Finite Element Analysis in Geotechnical Engineering: Application*, London, UK: Thomas Telford Publishing, 2001
[35] M.M. Badr, and Q.S.M. Shafiqu, “Predicting the performance of retaining structure under seismic loads by PLAXIS software,” *Journal of the Mechanical Behavior of Materials*, vol. 32, no. 1, pp. 1–9, 2023, https://doi.org/10.1515/jmbm-2022-0251.
[36] C.-N. Liu, Y.-H. Ho, and J.-W. Huang, “Large scale direct shear tests of soil/PET-yarn geogrid interfaces,” *Geotextiles and Geomembranes*, vol. 27, no. 1, pp. 19–30, 2009, https://doi.org/10.1016/j.geotexmem.2008.03.002.
[37] L.D. Wesley,”Soil compaction,” in *Fundamentals of soil mechanics for sedimentary and residual soils*, Hoboken, NJ, USA: John Wiley & Sons, Inc., 2009, pp. 391-404

[38] R. Proctor, “The design and construction of rolled earth dams”, *Engineering News Record*, vol. 111, no. 9, pp. 245–248, 1933.

[39] D. Fredlund, and H. Rahardjo, “Measurement of shear strength parameters,” in *Soil Mechanics for Unsaturated Soils*, Wiley, 1993, pp. 260-296.

[40] S. Yang, R. Lohnes, and B. Kjartanson, “Mechanical properties of shredded tires,” *Geotechnical Testing Journal*, vol. 25, no. 1, pp. 44–52, 2002, https://doi.org/10.1520/GTJ11078J.

[41] A. Edinçliler, G. Baykal, and A. Saygılı, “Influence of different processing techniques on the mechanical properties of used tires in embankment construction,” *Waste management*, vol. 30, no. 6, pp. 1073–1080 2010, https://doi.org/10.1016/j.wasman.2009.09.031.

[42] S. Youwai, and D.T. Bergado, “Strength and deformation characteristics of shredded rubber tire - sand mixtures,” *Canadian Geotechnical Journal*, vol. 40, no. 2, pp. 254–264, 2003, https://doi.org/10.1139/t02-104.

[43] D.P. Coduto, *Geotechnical Engineering: Principles and Practices*, New Delhi, Prentice Hall, 1999

[44] D.N. Humphrey, and T.C. Sandford, “Tire chips as lightweight subgrade fill and retaining wall backfill,” in *Proceedings of the symposium on recovery and effective reuse of discarded materials and by-products for construction of highway facilities*, 1993: US Department of Transportation, Federal Highway Administration, pp. 5–87.

[45] J.J. Tweedie, D.N. Humphrey, and T.C. Sandford, “Tire shreds as lightweight retaining wall backfill: active conditions,” *Journal of Geotechnical and Geoenvironmental Engineering*, vol. 124, no. 11, pp. 1061–1070, 1998, https://doi.org/10.1061/(ASCE)1090-0241(1998)124:11(1061).

[46] H. Hazarika, E. Kohama, and T. Sugano, “Underwater shake table tests on waterfront structures protected with tire chips cushion,” *Journal of Geotechnical and Geoenvironmental Engineering*, vol. 134, no. 12, pp. 1706–1719, 2008, https://doi.org/10.1061/(ASCE)1090-0241(2008)134:12(1706).

[47] M.A. Warith, E. Evgin, and P.A.S. Benson, “Suitability of shredded tires for use in landfill leachate collection systems,” *Waste Management*, vol. 24, no. 10, pp. 967–979, 2004, https://doi.org/10.1016/j.wasman.2004.08.004.

[48] H. Danso, D.B. Martinson, M. Ali, and J. Williams, “Effect of fibre aspect ratio on mechanical properties of soil building blocks,” *Construction and Building Materials*, vol. 83, pp. 314–319, 2015, https://doi.org/10.1016/j.conbuildmat.2015.03.039.

[49] C. Prasad, E. Nambiar, and B. Abraham, “Plastic fibre reinforced soil blocks as a sustainable building material,” *International Journal of Advancements in Research & Technology*, vol. 1, no. 5, pp. 42–45, 2012.

[50] S. Konda, S. Chinoori, B. Jangala, and P. Sharma, “An experimental study on the soil reinforced blocks,” *Materials Today: Proceedings*, vol. 52, pp. 1068-1072, 2021, https://doi.org/10.1016/j.matpr.2021.10.492

[51] J. Philip, “The theory of infiltration: 1. The infiltration equation and its solution,” *Soil Science*, vol. 83, no. 5, pp. 345–358, 1957.

[52] D.J. Varnes, “Slope movement types and processes,” *Special report*, vol. 176, no. 11, pp. 33, 1978.

[53] W. Bishop A, “The principal of effective stress,” *Teknisk Ukeblad*, vol. 39, pp. 859–863, 1959.

[54] G.W. Clough, and J.M. Duncan, “Finite element analyses of retaining wall behavior,” *Journal of the Soil Mechanics and Foundations Division*, vol. 97, no. 12, pp. 1657–1673, 1971, https://doi.org/10.1061/JSFEAQ.0001713.

[55] D.M. Potts, and A.B. Fourie, “The behaviour of a propped retaining wall: results of a numerical experiment,” *Géotechnique*, vol. 34, no. 3, pp. 383–404, 1984, https://doi.org/10.1680/geot.1984.34.3.383.

[56] R.J. Bathurst, and M.R. Simac, “Geosynthetic reinforced segmental retaining wall structures in North America”. *Proceedings of the Fifth International Conference on Geotextiles, Geomembranes and Related Products*, Singapore, September 5-9, 1994, pp. 1, https://doi.org/10.13140/2.1.4738.8160.

[57] J. Dam, M. Van den Oever, and E. Keijsers, “Production process for high density high performance binderless boards from whole coconut husk,” *Industrial Crops and Products*, vol. 20, no. 1, pp. 97–101, 2004, https://doi.org/10.1016/j.indcrop.2003.12.017.

[58] K. Moran, A. Gilbreath, M. Méndez, D. Lin, and R. Sutton, “Tire wear: Emissions estimates and market insights to inform monitoring design,” *SFEI Contribution*, vol. 1109, 2023.